Journal of Organometallic Chemistry, 475 (1994) 283–288

Interpenetrating organometallic polymer networks in heterogeneous catalysis: mild hydrogenation of *p*-nitrotoluene

B. Corain, M. Zecca and A. Biffis

Centro per lo Studio della Stabilità e Reattività dei Composti di Coordinazione, C.N.R., via Marzolo 1, I-35131 Padova, —c/o Dipartimento di Chimica Inorganica Metallorganica e Analitica, via Marzolo 1, I-35131 Padova (Italy)

S. Lora

Istituto di Fotochimica e Radiazioni d'Alta Energia, C.N.R., I-35020 Legnaro (Italy)

G. Palma

Dipartimento di Chimica Fisica, via Loredan 2, I-35131 Padova (Italy)

(Received January 20, 1994)

Abstract

A cross-linked organometallic macroporous copolymer (**P1**) and an interpenetrating organometallic polymer network (IOPN) material (**C1**), both based on the organometallic monomer *cis*-($PdCl_2$(CN CH_2)$_3$OC(O)CH=CH_2)$_2$) (**1**), are catalytically active and reusable in the mild and selective hydrogenation of *p*-nitrotoluene to *p*-toluidine in methanol, under ambient conditions. The IOPN catalyst **C1** is generated by the dispersion of a copolymer of **1** inside a macroporous poly-dimethylacrylamide-methylenebisacrylamide matrix to give an expectedly microporous organometallic matrix which exhibits a catalytic productivity quite similar to that displayed by **P1**. The productivity of both catalysts is comparable to that exhibited by commercial Pd/C under the same conditions, with **P1** and **C1** far superior in terms of separability and handiness.

Key words: Palladium; Polymer

1. Introduction

We have recently reported a novel strategy for the dispersion of metal centres inside insoluble organic matrixes [1–3]. The strategy is based on the generation of an organometallic copolymer (OC) inside the macro- and microporous domains of suitable preformed polymeric matrices (synthesis of interpenetrating organometallic polymer networks) [2]. In model experiments the OC was based on vinylferrocene as paradigmatic organometallic comonomer.

The employment of a catalytically relevant organometallic comonomer is the obvious next step for evaluating the relevance to catalysis of the IOPN strategy. The major predictable advantage of IOPN catalysts with respect to any traditional supported metal catalyst could be in the possibility of a wide choice of both organometallic component and synthetic support (*e.g.* lipophilic, hydrophilic, functional, chiral, *etc.*).

A copolymer of *cis*-$PdCl_2$(IPA)$_2$ (**1**) (IPA = 3-isocyanopropylacrylate) with dimethylacrylamide (DMAA) and methylenebisacrylamide (MBAA) (as the cross-linker) (**P1**) has been shown, in these laboratories [4], to be an active and reusable catalyst for the hydrogenation of phenylacetylene, benzaldehyde and nitrobenzene in ethanol and dichloromethane, under ambient conditions. This copolymer therefore appears to be a suitable candidate as the "guest" component of an IOPN catalyst based on a widely solvent-compatible [5] macro- and microporous support, such as poly(DMAA) crosslinked with 4% (mol/mol) MBAA (matrix **M**).

We report in this paper on the synthesis of an IOPN catalyst (**C1**) in which the OC is chemically close to **P1**,

Correspondence to: Dr. B. Corain.

0022-328X/94/$7.00
SSDI 0022-328X(94)24520-S

and on its catalytic activity in the hydrogenation of *p*-nitrotoluene in methanol and dichloromethane, under ambient conditions. In fact, **C1** is obtained by copolymerization of **1** with DMAA and MBAA within the macroporous domains of **M**. The results will be compared with those referring to **P1** and to a composite, prepared *ad hoc*, between the same OC and a commercially available microporous inorganic support (SiO_2, Daltosil 150). A popular commercial catalyst like Pd on carbon will also be tested in the same conditions for comparison.

2. Experimental section

2.1. Materials

MBAA and DMAA were obtained from Jannsen, Daltosil 150 was obtained from Serva, *p*-aminotoluene, *p*-nitrotoluene, MeOH and CH_2Cl_2 were supplied by Carlo Erba (RPE reagents). Dimethylformamide (DMF) was purchased from Aldrich. All the products were employed as received. Pd on carbon (5% w/w) was from Aldrich.

2.2. Apparatus

SEM and XRMA analyses were carried out by means of a Cambridge Stereoscan 250 EDX PW 9800 apparatus. A Shimadzu GC-8A gas chromatograph (FID detector) equipped with a SGE 25AQ3 capillary column (BP10, $\varnothing_{int} = 0.33$ mm, film thickness 0.5 μm, length 25 m) was employed for the analysis of the reaction mixtures in the catalytic tests. IR spectra were recorded with a Bio-Rad FTS7 PC spectrophotometer. Thermogravimetric analyses were carried out by means of a Perkin-Elmer TGS-2 microbalance. ESR spectra were recorded on a Bruker ER 200D X-band spectrometer. The elemental analyses (C, H, N) were carried out by means of a Carlo Erba 1106 Analyzer. Atomic absorption measurements (Pd) were performed with a Perkin-Elmer 3030 Atomic Absorption Spectrophotometer.

2.3. Synthesis of 1, M, P1, C1, Si1

1: Monomer **1** was prepared as described elsewhere [4].

M: DMMA (2.907 g) and MBAA (0.177 g) were mixed with water (3.434 g). Dioxygen was stripped by bubbling dinitrogen through the mixture, which was then injected dropwise into cooled (−78°C), dinitrogen saturated, petroleum ether. The frozen droplets were kept at low temperature during the irradiation with γ-rays from a ^{60}Co source (20.7 h, dose rate = 0.50 Gy s^{-1}). The polymer beads were recovered and allowed to warm to room temperature. They were repeatedly washed with methanol and diethyl ether and finally dried in an oven at *ca.* 80°C for some hours. The polymerization yield was quantitative. Elemental analysis: C 52.07; H 8.28; N 11.86%.

P1: This was obtained as described for **M**. The following amounts of chemicals were employed: **1**, 0.174 g; DMAA, 0.806 g; MBAA, 0.055 g; water, 0.583 g. The total radiation dose was the same as above. The polymerization yield was quantitative. Elemental analysis: C 50.10; H 7.90; N 10.74; Cl 1.92; Pd 2.61%.

C1: 0.259 g of **M** were swollen to incipient wetness, under a dioxygen free atmosphere, with a dinitrogen saturated solution of **1** (0.091 g), DMAA (0.164 g) and MBAA (0.016 g) in 0.173 g of DMF. The swollen beads were exposed to the γ-rays from a ^{60}Co source (50 h, dose rate = 0.50 Gy s^{-1}), at room temperature. The recovered material was washed with DMF, methanol, diethyl ether and finally dried *in vacuo*. The polymerization yield was quantitative. Elemental analysis: C 51.25; H 7.90; N 11.51; Cl 1.49; Pd 3.53%.

Si1: This was obtained by a similar procedure. 0.385 g of silica was flushed with dinitrogen and then soaked with a dinitrogen saturated solution of **1** (0.269 g), DMAA (0.330 g) and MBAA (0.027 g) in DMF (0.362 g). The impregnated particles were exposed to the γ-rays from a ^{60}Co source (32 h, dose rate = 0.50 Gy s^{-1}). The polymerization yield was not determined.

2.4. Catalytic tests

The catalytic runs were carried out in glass reactors (agitated at *ca.* 1 Hz) under batch conditions, at room temperature under dihydrogen (*ca.* 105 KPa). In a typical test, the catalyst was added to 10 ml of a solution of the substrate (1 M in methanol or dichloromethane). The analytical concentration of palladium was set to 5 mM and the amount of catalytic material was determined according to its metal load. The reaction mixture was saturated with dihydrogen through three freeze-thaw cycles with dihydrogen and kept under shaking for the required time. The course of the reaction was monitored by GC analysis (five samples of about 0.1 ml were taken at given times for each run).

2.5. Sample preparation for XRMA

A bead of polymeric material was embedded in a resin (Araldite) and the obtained block was cut with a round blade microtome. In this way, the great circle of the bead was uncovered and made available for scanning with the electron beam. Because of the relatively low mechanical strength of **C1**, its beads underwent occasional limited cracking while being cut. In these cases, artefacts (for instance, darker regions in the

distribution map of the observed element) could appear in the final micrograph, but they were clearly revealed by the concomitant SEM picture.

2.6. Sample preparation for ESR measurements

The matrix or catalyst particles (typically 30 mg) were swollen in *ca.* 1 ml of a *ca.* 10^{-4} M methanol solution of tempone (2,2,6,6-tetramethyl-4-oxo-1-oxylpiperidine) for one hour. This time was found to be sufficient for all the materials to reach the swelling equilibrium. The external liquid was then removed by quickly rubbing the swollen material on filter paper, and the sample was loaded into the ESR tube.

3. Results

3.1. Synthetic, morphological and analytical aspects

Matrix **M** is obtained in bead form (1.5–2 mm diameter) on the basis of an established procedure [6], which can be used to prepare hydrophilic or moderately lipophilic matrices possessing a fairly regular macroporosity. SEM analysis of **M** indeed shows a homogeneous distribution of macropores with an average pore diameter of $\approx 10^{-1}$ μm (Fig. 1a). TG analysis reveals thermal stability up to *ca.* 270°C, under dinitrogen.

The self-supporting catalyst **P1** is obtained as yellow-brown beads (2.5–3 mm diameter) with the same procedure as that employed for matrix **M**. The observed macroporosity of **P1** (Fig. 1b) is rather similar to that of **M**. Palladium and chlorine distribution have been confirmed [4] as quite homogeneous throughout the cross-section of the individual beads (Fig. 2a). The IR spectrum of **P1** clearly reveals the presence of the original organometallic unit as shown by a weak doublet at 2234 and 2200 cm^{-1}. TG analysis under dinitrogen reveals thermal stability up to *ca.* 200°C.

The γ-rays induced copolymerization of **1** with DMAA and MBAA in DMF inside matrix **M** occurs readily with almost quantitative yield. The observed metal content (3.53 *vs.* 3.92% w/w) suggests incomplete copolymerization of the organometallic comonomer. However, **1** is not a major component of the monomer mixture (about 17% w/w) and thus the above mentioned circumstance affects only slightly the overall polymerization yield. SEM analysis of the obtained IOPN material reveals a less porous structure with respect to **M** (Fig. 1c) and XRMA shows a fairly uniform distribution of palladium and chlorine throughout the composite beads (2–2.5 mm diameter) (Fig. 2b), which appear brown-yellow in colour. The IR spectrum of **C1** shows very clearly the presence of the *cis*-$PdCl_2(CN(CH_2)_3OC(O)CH{=}CH_2)_2$ monomeric units, which are unambiguously revealed by a weak doublet at 2234 and 2200 cm^{-1} and by the 1712 cm^{-1} carbonyl band of the ester group. TG analysis under dinitrogen reveals thermal stability up to 138°C.

A procedure identical in principle to that employed for obtaining **C1** was applied to silica particles (diameter = 0.1–0.2 mm; pore diameter = 20 nm; specific area = 275 m^2 g^{-1}; specific volume = 1.1 ml g^{-1}) but it led to a modest incorporation of palladium (1.97% w/w *vs.* an expected 6.21%). However, the resulting material, **Si1**, appears to be an organometallic copolymer-silica composite with a fairly homogeneous distribution of the metal centres (Fig. 3). The individual beads of

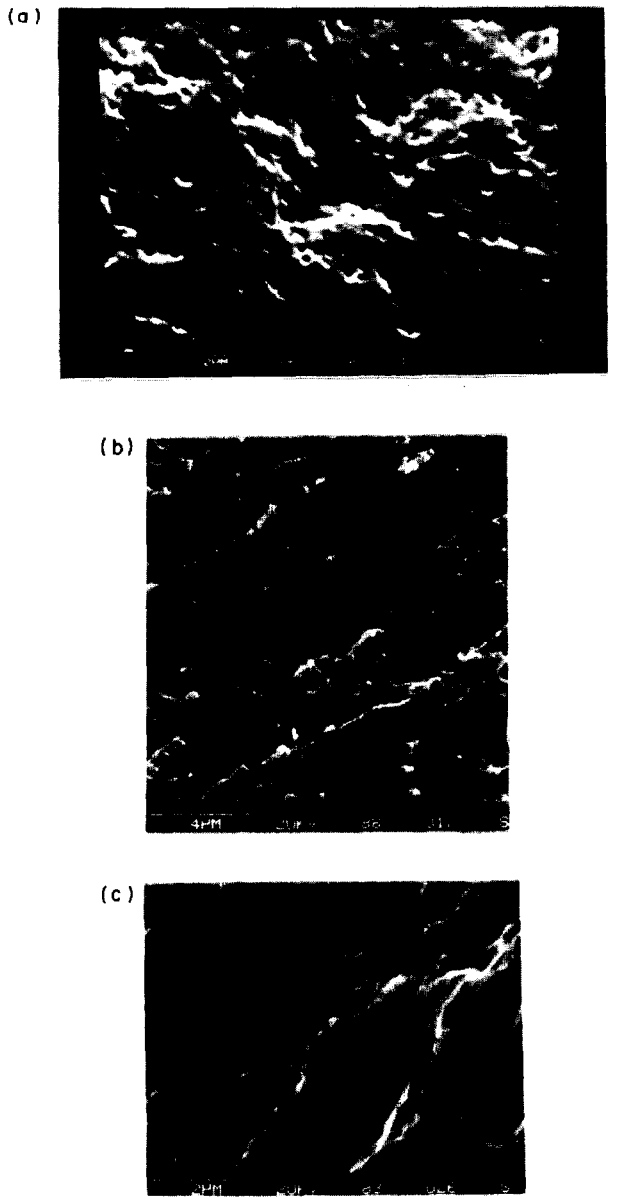

Fig. 1. SEM picture of self-supporting organometallic copolymer **P1** (a), of matrix **M** (b) and of molecular composite **C1** (c).

the material are pale yellow in colour and fairly transparent. The IR spectrum reveals a very weak doublet at *ca.* 2240 and 2200 cm^{-1} and a weak band in the ester carbonyl region, indicating again the incorporation of the *cis*-$PdCl_2(CN(CH_2)_3OC(O)(CH{=}CH_2))_2$ monomeric units.

3.2. Catalytic results

P1 and **C1** are both catalytically active in methanol ([*p*-nitrotoluene] = 1 M, [Pd] = 5 10^{-3} M (analytical), at 20°C and atmospheric pressure) in the selective reduction of *p*-nitrobenzene to *p*-toluidine. The composite **Si1** is completely inactive in methanol and dichloromethane. No evidence of hydrogenation of *p*-nitrotoluene in the presence of **P1** or **C1** in dichloromethane is observed.

Both catalysts are very easily reusable (**P1** was recycled five times and **C1** three times) upon simple decantation of the final suspension, without any loss of activity. They require an evident activation time during the first run (*ca.* 24 h for the quantitative conversion of the substrate), after which process they are equally productive, with conversion times of about seven hours. The conversion (% mol/mol) *vs.* time (min) profiles are straight lines with slopes of 0.19 (**P1**) and 0.16 (**C1**). Reference experiments performed with commercial Pd/C, under identical conditions, also give a straight line profile in the early stages of the reaction, with a comparable slope (0.68). However, as the reaction proceeds, some evidence of kinetic control is found. No reusability experiments have been attempted with this catalyst.

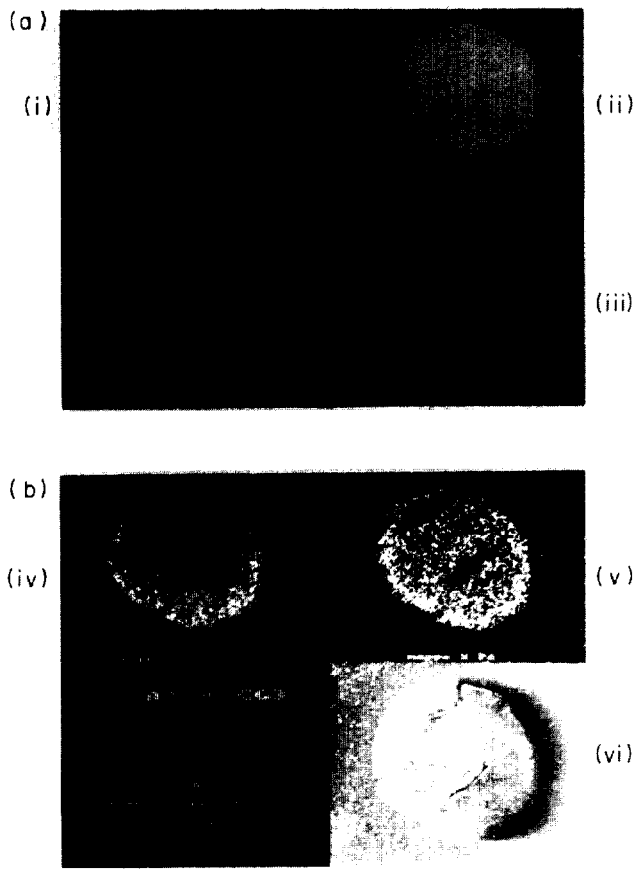

Fig. 2. XRMA scanning picture of a cross-section of a bead of the self-supporting organometallic copolymer **P1** (a, i = Cl; ii = Pd; iii = SEM) and of the molecular composite **C1** (b, iv = Cl; v = Pd; vi = SEM). The darker regions apparent in the scanning picture are artefacts due to surface defects (see Experimental section).

Fig. 3. XRMA scanning picture of **Si1**. Pd (iii) and Cl (ii) distribution appears to be fairly regular throughout the silica beads cross sections. Silicon distribution (i) and SEM (iv) are also presented.

For both **P1** and **C1** catalysts the colour of the catalytic material turns to black and the IR spectrum of the recovered catalyst reveals the complete disappearance of the ν(CN) band of the *cis*-$PdCl_2(CN{-}R)_2$ unit. Moreover, XRM analysis of the material, as well as of **Si1**, reveals no substantial change in palladium content and distribution, while on the contrary a very marked reduction of chlorine content is observed. In contrast with this observation, both catalysts maintain colour, XRMA patterns and IR spectrum after the attempted catalytic runs in dichloromethane. Apparently, the lack of catalytic activity is paralleled by lack of reduction of Pd^{II} to Pd^0, which is likely to occur according to Scheme 1.

3.3. Evaluation of molecular accessibility in M, P1 and C1 after swelling in methanol

The rotational mobility [3] of paramagnetic probes dissolved in a solution confined inside the microporous domains of a given material is a sensitive function of the microviscosity of the medium [7], which, in turn, strongly depends on the actual volume of the nanometric sized cavities found in this type of material [8,9]. Thus, the smaller the cavity volumes the greater the

local viscosity and the lower the rotational mobility of the employed probe. This molecular feature of a given probe molecule is conveniently expressed by the rotational correlation time [3] τ (ps), which can be very easily measured from simple features of the ESR spectrum of the paramagnetic probe. If the material to be examined is a cross-linked polymer this ESR procedure will produce two major pieces of information: i) estimated concentration of polymer chains [3] (*i.e.* indirectly, of relative cavity volumes), and ii) actual accessibility of the micropores to probes possessing well defined molecular sizes.

In this work we have chosen the nitroxide stable radical tempone as paramagnetic probe (molecular volume *ca.* 0.2 nm^3), and the relevant τ values are collected in Table 1.

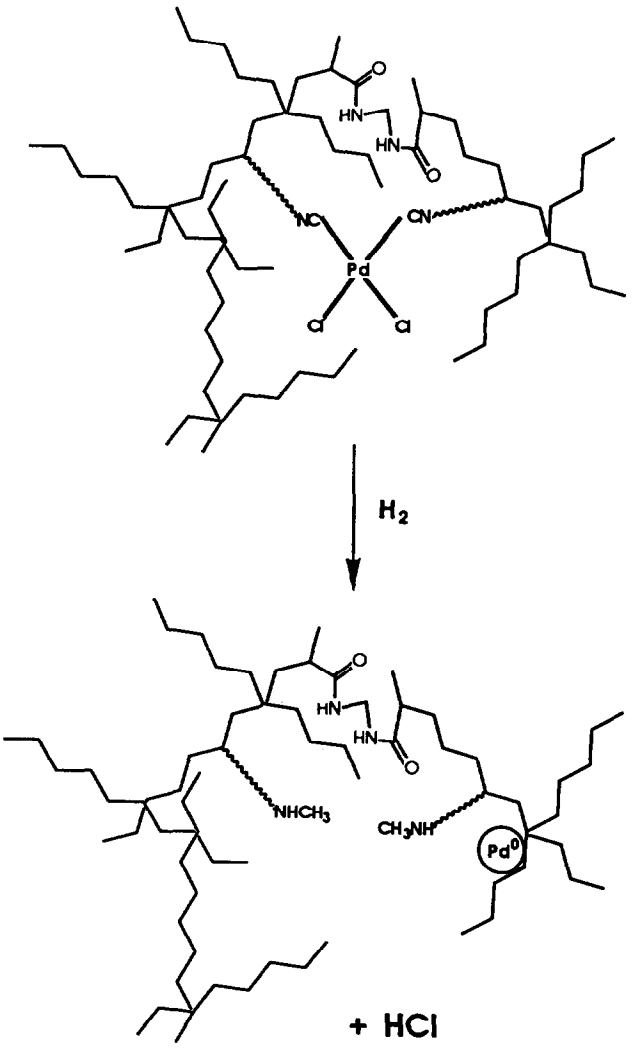

Scheme 1. Schematic description of the activation of **P1** and **C1**.

TABLE 1. Rotational correlation time τ (ps) of tempone dissolved in methanol and confined inside various materials, at 293 K. The τ value in bulk methanol is 25 ps

Sample	P1	C1	M
Before activation	152	316	98
After activation	154	250	–
Recycle 1	129	265	–
Recycle 2	118	284	–
Recycle 3	121	287	–
Recycle 4	–	–	–
Recycle 5	138	–	–

The ESR spectrum of the probe inside the materials investigated appears quite uncomplicated and exhibits the expected triplet, with sharp bands typical of relatively freely rotating nitroxide molecules [3, 8, 9]. It is worth underlining that this pattern does exclude any adsorption ("immobilization") of the reporter on the polymer chains of the macromolecular networks. The rotational mobility of tempone "free" to move in bulk methanol undergoes an appreciable decrease (τ increases *ca.* four times) when its solution is confined within the macro- and microporous domains of matrix **M**, thus indicating that the solvent inside the matrix is appreciably, but not dramatically more viscous [7] than under bulk conditions. A similar rotational mobility is observed inside **P1** with respect to **M**, in agreement with the similarity of their morphology (SEM data) and chemical nature. On the other hand, an (expected) decrease of mobility is observed on going from **M** to **C1**, *i.e.* from a macroporous to an expectedly microporous matrix, although the difference is not as marked as one would have expected on the basis of simple chemical intuition.

The data of Table 1 reveal that no marked overall matrix structural changes appear to be associated with the activation of both catalysts, which is paralleled by the reduction of Pd^{II} to Pd^0 and by a certain degree of reversal of crosslinking (see Scheme 1). This however seems to be the reason for the observed slight decrease in the correlation times for **C1** (Table 1).

4. Discussion and conclusions

The copolymerization of the organometallic comonomer **1** with DMAA and MBAA occurs successfully inside the macroporous domains of preformed designed (organic and inorganic) supports. Metal distribution is even and the chemical identity of the organometallic chromophore appears to be guaranteed.

Evaluation of molecular accessibility by a probe of substantial size such as tempone and of rotational mobility inside the structural domains of the composite

C1 reveals that the overall macromolecular structure of the IOPN does not prevent molecular mobility of species moving to and from the metal centres. Quite in line with this observation, IOPN **C1** exhibits a catalytic productivity very similar to that of an expectedly more viable related material such as **P1** and of a popular catalyst like Pd/C. Unfortunately, the conversion profiles reveal that the data reported here were obtained under a diffusion regime, and this circumstance prevents a comparison of real catalytic activities. However, in spite of this conceptual limitation, the total lack of activity of the composite **Si1** does indirectly stress the accessibility of catalyst **C1** to reagents and products. In fact, we can imagine that the dispersion of the OC inside the micropores of Daltosil 150 will be followed by reduction of metal in methanol under hydrogen to give metal crystallites which are located inside micropores "jammed" by poly-DMAA chains, thus being obviously inaccessible through the rigid silica structure. Therefore, only the external part of the catalyst particles would be potentially, although in fact not sufficiently, active. On the contrary, the metal crystallites generated inside **C1** do not suffer this trapping effect, being surrounded by a swollen and fairly accessible polymer network.

Finally, the lack of activity observed for both **P1** and **C1** in dichloromethane is clearly attributable to the lack of reduction of Pd^{II} to Pd^{0} (lack of activation), as revealed by IR observations and XRMA.

Acknowledgments

This work was partially supported by Progetto Finalizzato Chimica Fine II, C.N.R. - Rome and by MURST funding (40%). We thank Prof. G. Favero for TG data.

References

1 R. Arshady, B. Corain, S. Lora, G. Palma, U. Russo, F.O. Sam and M. Zecca, *Adv. Mater., 2* (1990) 412
2 B. Corain, K. Jerabek, S. Lora, G. Palma and M. Zecca, *Adv. Mater. 4* (1992) 97
3 B. Corain, C. Corvaja, S. Lora, G. Palma and M. Zecca, *Adv. Mater., 5* (1993) 367
4 B. Corain, F.O. Sam, M. Zecca, S. Lora and G. Palma, *Angew. Chem., Int. Ed. Engl., 29* (1990) 384
5 R. Arshady, *Adv. Mater., 3* (1991) 182 and references therein
6 R. Arshady, M. Basato, B. Corain, L. Della Giustina, S. Lora, G. Palma, M. Roncato and M. Zecca, *J. Mol. Catal., 53* (1989) 111
7 G. Nimtz, in H.E. Stanley and N. Ostrowsky (eds.), *Correlation and Connectivity*, NATO ASI Series, *118*, Kluwer, Dordrecht, p. 225
8 G. Martini and L. Burlamacchi, *Chem. Phys. Lett., 41* (1976) 129
9 G. Martini, M.F. Ottaviani and M. Romanelli, *J. Colloid Interface Sci., 115* (1987) 87
10 A.G. Ogston, *Trans. Faraday Soc., 54* (1958) 1754
11 B. Corain, M. Basato, M. Zecca, G. Braca, A.M. Raspolli Galletti, S. Lora, G. Palma and E. Guglielminotti, *J. Mol. Catal., 73* (1992) 23